AD-A184 928 PHOTOCURRENT GENERATION FROM BASIC METALS UTILIZING A SHORT PULSED ARF EXCIMER LASER(U) NAVAL POSTGRADUATE SCHOOL MONTEREY CA T J RINGLER SEP 87 1/1

UNCLASSIFIED F/G 9/3 NL

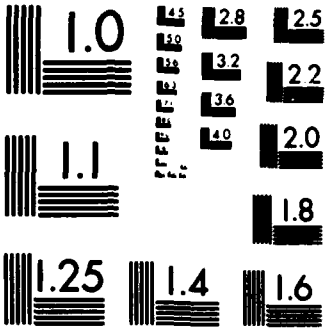

MICROCOPY RESOLUTION TEST CHART
NATIONAL BUREAU OF STANDARDS-1963-A

(2)

NAVAL POSTGRADUATE SCHOOL

Monterey, California

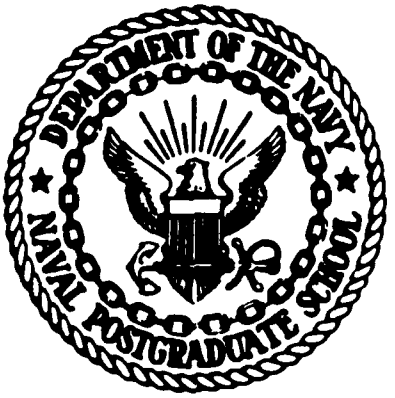

THESIS

PHOTOCURRENT GENERATION FROM BASIC METALS, UTILIZING A SHORT PULSED ArF EXCIMER LASER

by

Thomas J. Ringler

September 1987

Thesis Advisor: F. R. Buskirk

UNCLASSIFIED

ADA184928

SECURITY CLASSIFICATION OF THIS PAGE

REPORT DOCUMENTATION PAGE

1a REPORT SECURITY CLASSIFICATION: UNCLASSIFIED	1b RESTRICTIVE MARKINGS
2a SECURITY CLASSIFICATION AUTHORITY	3 DISTRIBUTION/AVAILABILITY OF REPORT: Approved for public release; distribution is unlimited.
2b DECLASSIFICATION/DOWNGRADING SCHEDULE	
4 PERFORMING ORGANIZATION REPORT NUMBER(S)	5 MONITORING ORGANIZATION REPORT NUMBER(S)
6a NAME OF PERFORMING ORGANIZATION: Naval Postgraduate School; 6b OFFICE SYMBOL (If applicable): 61	7a NAME OF MONITORING ORGANIZATION: Naval Postgraduate School
6c ADDRESS (City, State, and ZIP Code): Monterey, California 93943-5000	7b ADDRESS (City, State, and ZIP Code): Monterey, California 93943-5000
8a NAME OF FUNDING/SPONSORING ORGANIZATION; 8b OFFICE SYMBOL (If applicable)	9 PROCUREMENT INSTRUMENT IDENTIFICATION NUMBER
8c ADDRESS (City, State, and ZIP Code)	10 SOURCE OF FUNDING NUMBERS: PROGRAM ELEMENT NO; PROJECT NO; TASK NO; WORK UNIT ACCESSION NO

11 TITLE (Include Security Classification): PHOTOCURRENT GENERATION FROM BASIC METALS, UTILIZING A SHORT PULSED ArF EXCIMER LASER

12 PERSONAL AUTHOR(S): Ringler, Thomas J.

13a TYPE OF REPORT	13b TIME COVERED	14 DATE OF REPORT (Year Month Day)	15 PAGE COUNT
Master's Thesis	FROM ____ TO ____	1987 September	61

16 SUPPLEMENTARY NOTATION

17 COSATI CODES			18 SUBJECT TERMS (Continue on reverse if necessary and identify by block number)
FIELD	GROUP	SUB-GROUP	Photoelectric Effect ArF Excimer Laser Photoemission Quantum Efficiencies for Metals

19 ABSTRACT (Continue on reverse if necessary and identify by block number)

An excimer laser used to produce "cold" photoelectrons from common metal surfaces offers an improvement over a standard heated (thermionic) cathode electron source. Photoelectrons accelerated across an anode cathode gap were observed under both space charge limited and emission limited conditions. Temporal characteristics of the resulting electron beam showed fast rise times of 3-5 nano seconds (ns) for space charge limited and 8-12ns (full width half maximum) for emission limited cases. Spatial characteristics of the output pulse shape revealed a classic clipped peak amplitude in the space charge pulse but identical characteristics in the emission limited pulse output. Both types of emission produced large current densities up to 91 amps/cm². Varying the cathode metal used for the photocathode indicates Zinc (Zn) produced the largest current density, and therefore, the highest quantum efficiency in both space charge and emission limited cases.

20 DISTRIBUTION/AVAILABILITY OF ABSTRACT	21 ABSTRACT SECURITY CLASSIFICATION
☒ UNCLASSIFIED/UNLIMITED ☐ SAME AS RPT ☐ DTIC USERS	UNCLASSIFIED
22a NAME OF RESPONSIBLE INDIVIDUAL: Prof. E. R. Pugh/mk	22b TELEPHONE (Include Area Code) / 22c OFFICE SYMBOL: 61Bs

DD FORM 1473, 84 MAR — 83 APR edition may be used until exhausted. All other editions are obsolete.

SECURITY CLASSIFICATION OF THIS PAGE

fgcm

UNCLASSIFIED

ABSTRACT

An excimer laser used to produce "cold" photoelectrons from common metal surfaces offers an improvement over a standard heated (thermionic) cathode electron source. Photoelectrons accelerated across an anode cathode gap were observed under both space charge limited and emission limited conditions. Temporal characteristics of the resulting electron beam showed fast rise times of 3-5 nano seconds (ns) for space charge limited and 8-12ns (full width half maximum) for emission limited cases. Spatial characteristics of the output pulse shape revealed a classic clipped peak amplitude in the space charge pulse but identical characteristics in the emission limited pulse output. Both types of emission produced large current densities up to 91 amps/cm^2. Varying the cathode metal used for the photocathode indicates Zinc (Zn) produced the largest current density, and therefore, the highest quantum efficiency in both space charge and emission limited cases.

ACKNOWLEDGEMENT

With great appreciation to Dr. D. C. Moir and Dr. S. W. Downey of the Los Alamos National Laboratory, for their guidance, patience and long hours assisting with the Poloroid pictures.

To my wife Leslie for the many hours assisting on the computer.

investigated fairly recently. Both synchotron radiation made available in the 1960's and development of the excimer laser, which can produce consistent high intensity, monochromatic light in the ultraviolet region have permitted further research in this region of shorter wavelengths. Recent advances in pulsed excimer lasers make it possible to achieve high photon fluxes of about 10^{16} photons per square centimeter per second (photons/cm^2·sec), for unfocused beams in the UV region. These recent advances have sparked renewed interest in photoelectron generation using common metals, even though metals in general produce very low quantum efficiencies.

This thesis investigates the relative quantum efficiencies of nine common metals for the production of photoelectrons. An Argon Florine (ArF), excimer laser is used as the illuminating photon source. The results are to be used in determining the best cathode material for construction of an improved electron injection source for the Pulsed High-Energy Radiographic Machine Emitting X-Rays (PHERMEX) accelerator currently in use at the Los Alamos National Laboratory.

associated with metals that have lower surface work functions. Furthermore, electrons emitted from thermionic cathodes demonstrate a large spectrum of kinetic energies, and more importantly, show a wide variance in the radial components of momentum that are not parallel to the direction of beam propagation. This means the electrons tend to spread out in all directions as they are emitted. Efficient utilization of this type of electron beam may be constrained unless further beam enhancement methods such as focusing or aperture restrictions are incorporated to remove the undesired divergence effects of the electron beam.

2. Field Emission Cathodes

This process utilizes intense electric fields with threshold strengths on the order of 1.0×10^6 to 5.0×10^7 Volts/Meter (V/M) [Ref. 1] to extract electrons, normally from a tungsten cathode surface. The cathode material is usually unheated, but can also be heated to further reduce the surface work function. In general, the intense electric fields shift the surface potential energy barrier to a lower level where valence electrons in the bulk metal have enough internal energy to tunnel out and escape. An electron beam produced by this method has a large radial momentum component associated with the emitted electrons and usually needs to be focused or restricted by a series of apertures to remove the divergence effects. Use of a restrictive series of apertures may result in a several fold reduction in the beam intensity. This system is inefficient, requiring large amounts of energy to generate the electric fields needed for electron extraction and is complicated to construct as compared to thermionic emitters.

that quantum efficiencies will not exceed 10^{-2} [Ref. 2]. Metal quantum efficiencies are usually in the 10^{-4} region. At low incident photon energies (6.4 e.v.), quantum efficiency is calculated assuming one incident photon will generate only one photoelectron, and therefore, its value will not exceed unity. At higher incident photon energies, where secondary electron production may occur within the metal, quantum efficiencies higher than unity may be obtained.

4. Elaborate Cathodes

In addition to simple metal cathodes there are a number of much more elaborate cathodes [Refs. 2, 3] that have been constructed over the last 10 years using exotic combinations of several elements. These usually entail the use of an active alkali metal layer on top of, or combined with, one or two other metals. These cathodes provide very high quantum efficiencies and have good emitted electron momentum characteristics. Current densities up to 200 amps/cm^2 [Ref. 4] with quantum efficiencies as high as 0.2 to 0.3 have been achieved. This is one order of magnitude better than can be achieved by simple metal cathodes. However, these systems pay a price in their complexity. They generally require surgically clean cathode surfaces and suffer intense degradation due to surface "poisoning" from vacuum chamber contaminants. Ultra-high vacuums, on the order of 10^{-10} torr must be maintained. The additional effort required to maintain these systems is an extreme disadvantage.

Of course, there are hybrid combinations of these three types of emitters that may provide improved efficiencies. The addition of thermionic heating in conjunction with field emission or photoelectron

pulse associated with emission limited flow and the "clipped" photocurrent pulse shape associated with space charge limited flow. When emission limited, photoelectrons do not interfere to any great extent with each other as they are emitted. The pulse shape is controlled by the shape of the input laser pulse. Space charge on the other hand, means electron production is great enough to cause those electrons already emitted to interfere with those that are being emitted. The pulse shape in space charge is clipped when electrons outside the metal surface build to a level where they prevent other electrons from emerging. Electron bunches can be generated in repeatable fashion with either of these specific pulse shapes by increasing or decreasing the laser beam power output. For low laser power conditions, a Gaussian shaped output can be obtained. At relatively large power outputs, where the cathode is driven into a space charge limit, a clipped pulse shape is observed.

C. TEMPORAL CHARACTERISTICS

The major advantage of laser produced electrons is the near "instantaneous" production of electrons from photon irradiation of a photocathode material. Following photon incidence, electrons are raised to excited levels within the metal after sub-pico second time delays. This allows direct control of the output pulse length by changing the length of the laser input pulse. It also allows high pulse repetition rates to be achieved when excimer laser pulse technology achieves laser repetition rates in the kilo Hertz region. Pulses observed in this research showed rise times of 8-12 nano seconds (ns) when operating in

III. EXPERIMENTAL PROCEDURE

The experiment was designed with simplicity in mind so that further research or a larger scale-up of the photocathode assembly could maintain the same simplicity in construction, reliability, cathode material availability and remain within low monetary constraints. The experimental apparatus for the generation of photoelectrons is shown in Fig. 2.

A. LASER/OPTICAL DESCRIPTION

The excimer laser used as a photon source was an "off the shelf" LAMBDA-PHYSIK EMG-150T. This gas filled laser can be used with either Argon Florine (ArF) or Krypton Florine (KrF) gas to produce an emitted laser beam in the ultraviolet end of the spectrum. Specifically, it can be tuned to either 193.4 nanometers (nm) or 248.0 nm wavelengths respectively. For this experiment, the laser was used in the ArF mode, producing photons with an energy of 6.4 electron volts (e.v.) per photon. The laser was pulsed at 2-3 Hertz (Hz) while determining data, but was capable of repetition rates of several tens of Hz. The laser was mounted, along with most other equipment, on a large optical table. The vacuum chamber, with a volume of about 10 liters, contained the target cathode and collector assembly. It was mounted separately on the floor at the end of the optical table to allow a Cryogenic, Cryo-Torr-8 vacuum pump to be attached as an integral part of the target chamber.

As the laser beam exited the excimer laser case it was translated 18 inches lower than the exit height, via two quartz plates adjusted at 45 degrees to the beam path to create a parallel beam path. The quartz plates were 98% reflective for the tuned laser wavelength of 193.4 nm. Translating the path allowed final beam alignment into the vacuum chamber and onto the cathode surface. Additional fine adjustments of the target chamber position permitted the photon beam to traverse internal apertures within the vacuum chamber. One drawback of the photon beam produced by the excimer was the non-circular and the non-homogeneous intensity composition over the beam's roughly elliptical cross section. To obtain a more uniform beam, an adjustable circular aperture was positioned just after the 45 degree reflecting plates and prior to the laser attenuator to allow selection of a circular portion of the beam with fairly uniform intensity characteristics. This also narrowed the beam, allowing it to pass through a NRC Model 935-16 Laser Variable Attenuator, reducing internal scattering and unwanted reflections. A variable attenuator was used to obtain data in the emission limited electron production region. For most emission limited data, intensity reductions on the order of 100 in laser beam power were required. The beam was then passed through a 50% reflecting quartz plate to produce a split beam. One portion was passed to an EGG FND-100Q Ultra Fast silicon photodiode used to monitor the laser pulse shape while the other portion of the beam was passed through a Suprasil entrance window and into the vacuum chamber. The Suprasil quartz window creates the standard 8% loss in transmission due to reflection. A second silicon photocell was used to monitor (from laser beam

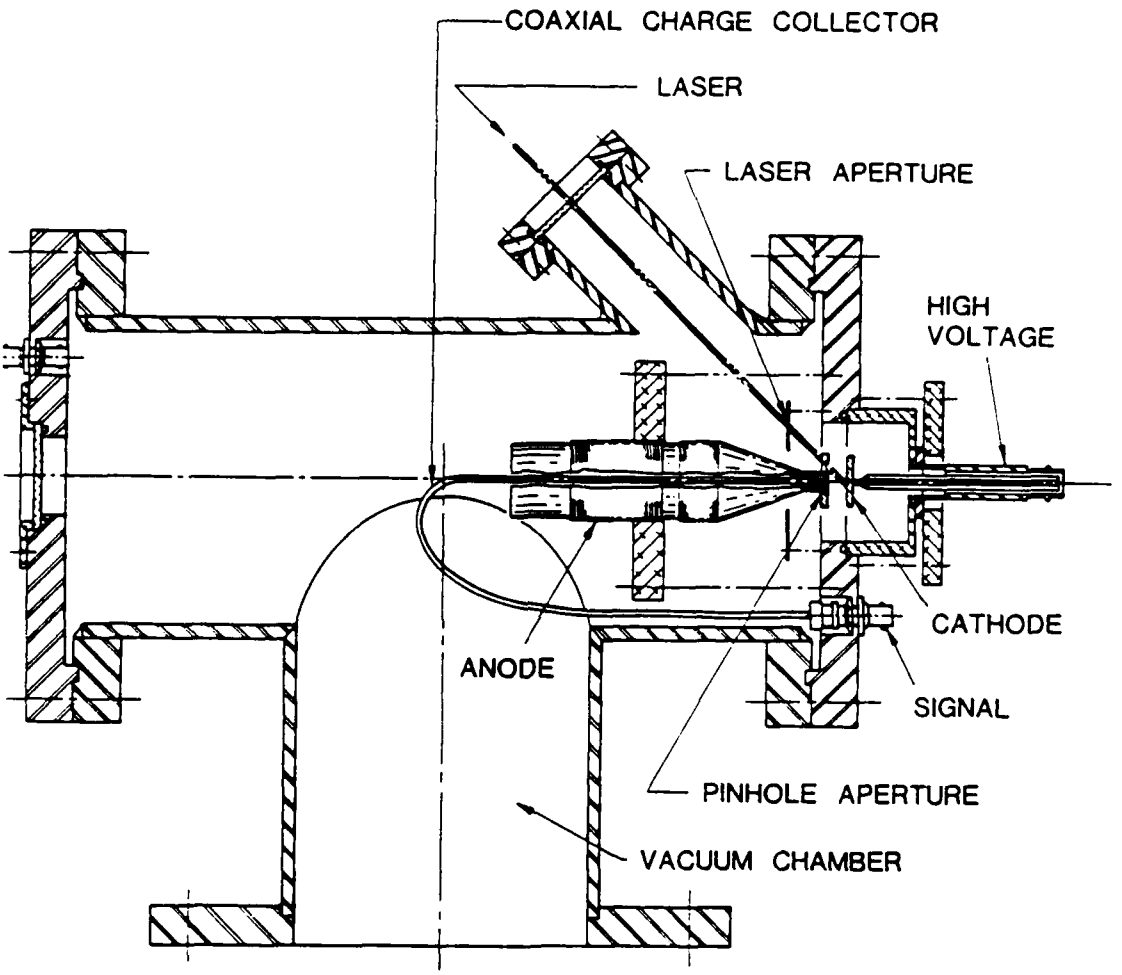

Figure 3. Initial Experiment Vacuum Chamber and Cathode Target.

substituted with another and data sets repeated at 5KV, 10KV, and 20KV. When some of the higher efficiency cathodes were used, they showed only space charge limited flow at 5KV. For these cathode materials, data points were also taken at 15KV. Photos were needed to "freeze" pulses for later analysis. Pulses on the photos were subjectively evaluated for pulse shape (to determine emission or space charge limit). Measurements were made of the peak amplitude, amplitude at full width half maximum (FWHM), time base for the input laser pulse and the photocurrent output, and time base at the FWHM point for the input and output pulses. This information was then manipulated by a computer program written to reduce the data, and determine current density, power per pulse and quantum efficiencies.

predominately a volume effect has been argued for many years. Where earlier investigations tended to indicate a volume effect, more recent investigations [Ref. 5] and the current trend in relavent information indicates that the surface effect is the main source of photoelectrons. One of the most general and widely accepted theories up through the early 1970's has been the so called "three step" process originally proposed in the 1960's by C. N. Bergland and W. E. Spicer [Refs. 6, 7]. This basic model varies depending on whether the cathode material being considered is a metal or a semiconductor. In general, this section discusses aspects that relate to simple metals unless otherwise specified.

C. THREE-STEP PHOTOEMISSION CONCEPT

The three-step process considers a photon of energy $\hbar\omega$, to interact with, and transfer momentum to, a single electron in the metal. According to basic theories generated in the early 1900's by P. Drude, metals are considered to contain a free flowing "sea of electrons" which exist in thermal equilibrium with the atoms of the metal [Ref. 8]. Incident photons excite this sea of electrons by momentum transfer that imparts enough energy to allow some to escape from the metal.

In step one of the three-step process (Fig. 4a), photon energy is totally transferred to a single electron at a depth (within a metal) ranging up to several hundred angstroms. The penetration depth is usually comparable to the electromagnetic radiation wavelength associated [Ref. 9] with the illuminating photon. Certainly, in metals at the frequencies associated with ultraviolet light, "photons have

towards the metal surface to enable them to "escape" as photoelectrons. In addition, even though an excited electron may have enough total energy when it arrives within range of the surface, the critical aspect of its momentum is the component perpendicular to the surface.

In step three of the three-step process (Fig. 4c), if the final perpendicular momentum component is greater than or equal to that required to break through the surface potential barrier (i.e. the work function of the metal) then the excited electron will escape and be emitted as a photoelectron into the adjoining medium (a vacuum for this experiment). This emitted electron may have any kinetic energy (K.E.),

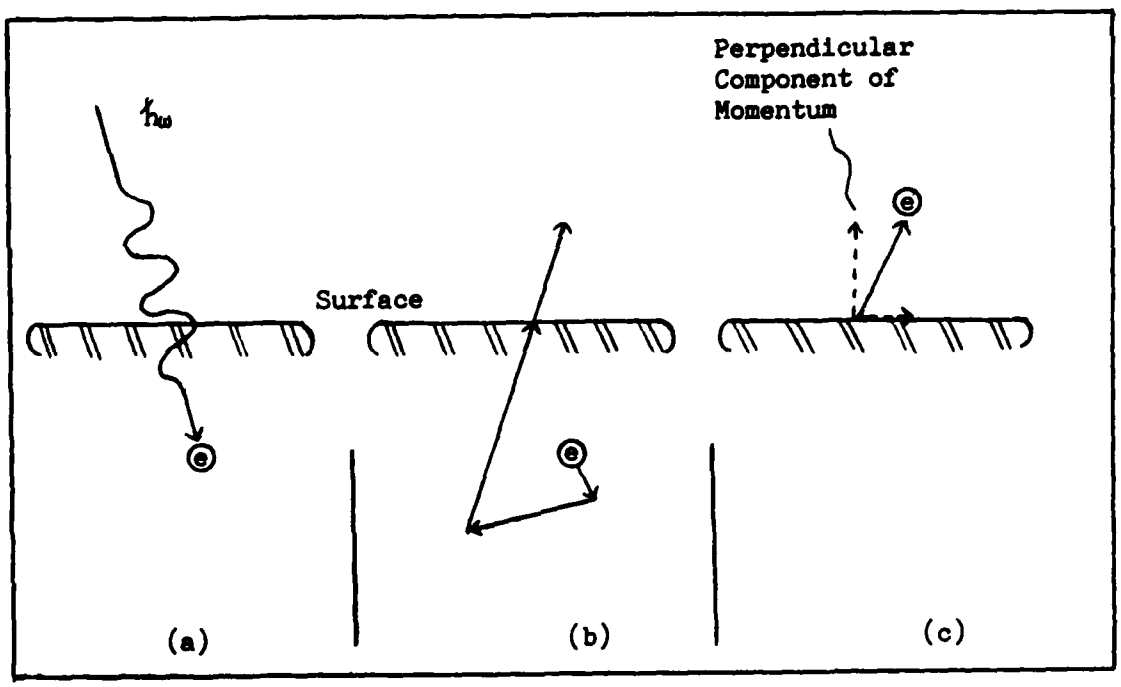

Figure 4. Three-Step Process of Photoelectron Emission: (a) Photon Energy is Totally Absorbed by Single Electron Within Metal; (b) Excited Electron May Undergo Multiple Collisions; (c) Electron Will Escape if Perpendicular Component of Momentum at Surface is Greater Than or Equal to Metal Work Function.

metal surface as shown in Fig. 5. Although not fully understood, this increased absorption is thought to be due to surface phonon coupling.

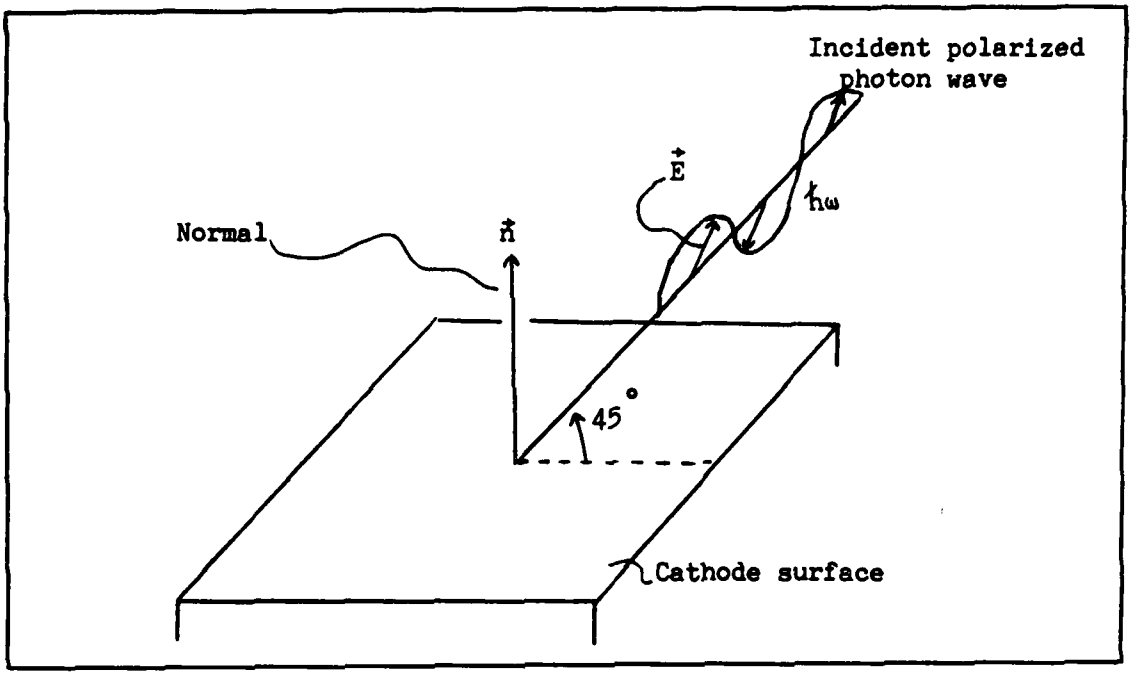

Figure 5. Optimal Geometry for Most Efficient Coupling of Polarized Laser Beam into Metal Cathode Surface.

2. Surface Contamination

In the three-step theory we assume a pure metal surface. In practice, emission is affected by the absorbate layer on the metal surface due to chemisorbtion (chemical interaction with the surface). This chemisorbtion may significantly alter photoemission, by adding or subtracting from the basic work function of the pure metal. This produces a larger or smaller observed work function which in turn will decrease or increase the number of emitted photoelectrons. A monolayer of adsorbed gases will form rapidly in all but the very highest vacuums.

above the metal. Additionally, surface roughness will affect the electron beam quality by producing greater divergence of the emitted photoelectrons. It has been proposed that better beam quality (by a factor of five) [Ref. 14] might be obtained by operating a photocathode in the space charge limited region vice the emission limited region. This is due to the greater divergence of emitted electrons from emission limited protuberances, whereas in the space charge limit case, the strong electric fields created by the space charge reduces the radial components of momentum that cause divergence.

E. THE SCHOTTKY EFFECT

The Schottky effect [Refs. 10, 15] is defined as an increase in electron emission (i.e. current) caused by the increasing electric field strength applied between the anode and cathode. Under the influence of an applied electric field, photoelectrons are removed from the area directly above the metal surface immediately. This allows higher photocurrents to be obtained because electrons are not being retarded by the electron cloud which builds up just above the surface. The Schottky effect creates an apparent decrease in the metal cathode surface work function and an apparent increase in the quantum efficiency. The work function is decreased by an amount:

$$\Delta\phi = -C(eE)^{0.5}$$

where E, e and C are respectively the electric field strength in kilo-Volts, the charge on an electron and a constant. This apparent

V. EXPERIMENTAL RESULTS AND DISCUSSION

The preliminary experiment objective was to determine whether current densities greater than 20-30 amps/cm^2 could be achieved from a laser driven cold photocathode. This value was chosen as a threshold because it is the present capability of the thermionic electron gun in operation at the Los Alamos PHERMEX accelerator. A goal of 50 amps/cm^2 was desired to allow a 100% improvement in the capacity of the present PHERMEX thermionic electron source. In addition, a simple laser driven cold cathode electron source would offer a vast improvement in simplicity and maintenance. Results of the initial investigation in April 1986 [Ref. 16], demonstrated the feasibility of this improvement with experimental current densities of 50-70 amps/cm^2 achieved in emission and space charge limited regions for a copper cathode. Further investigation, and the primary objective of this thesis, was directed towards comparing electron production from several metals to determine which cathode material would produce the highest quantum efficiency.

A. CATHODE MATERIALS AND WORK FUNCTIONS

Nine different metal cathode surfaces were used for this experiment. Eight samples were stock metals that had been diamond machined to a 2.54 cm diameter disk that was 0.40 cm thick. The ninth sample was a copper cathode base that was plated with 1000 Å of gold. In general, metals were of high purities exceeding 99%. After machining, no further attempt was made to highly polish the surface or remove surface

experimental determination of work functions. Accepted values [Ref. 2] listed in Table I, were determined from several techniques, which include both photoemission and thermionic emission. The conditions established for vacuum, temperature, surface contamination, metal purity, metal crystal orientation, surface or bulk emission, ect., all effect the ultimate assignment of a work function value. Therefore, these values are guidelines and should not be used for absolute comparisons unless they are all determined under exactly the same conditions by the same experimental procedure.

Thirdly, the metal work functions spanned only 1.23 volts between the nine metals tested. Most varied only several tenths of a volt between them. It was not possible under the accuracy conditions established in this experiment to determine if work functions had a direct effect on the relative quantum efficiencies.

TABLE I

RELATIVE QUANTUM EFFICIENCY DETERMINATIONS

Q.E. ORDER	CATHODE METAL (10 KV)	WORK FUNCTION (e.v.)	CATHODE METAL (15 KV)*	CATHODE METAL (20 KV)
1	Zinc (Zn)	-- 4.24	Sn	Zn
2	Tin (Sn)	-- 4.50	Zn	Al
3	Aluminum (Al)	-- 4.20	Cu	Cu
4	Copper (Cu)	-- 4.54	Al	Au
5	Gold (Au on Cu)	-- 4.92	Au	Ni
6	Magnesium (Mg)	-- 3.68		Sn
7	Nickel (Ni)	-- 5.01		Mg
8	Stainless Steel(s-s)	-- 4.77		s-s
9	Tungsten (W)	-- 4.69		W

* Incomplete data obtained for comparison, on metals not listed.

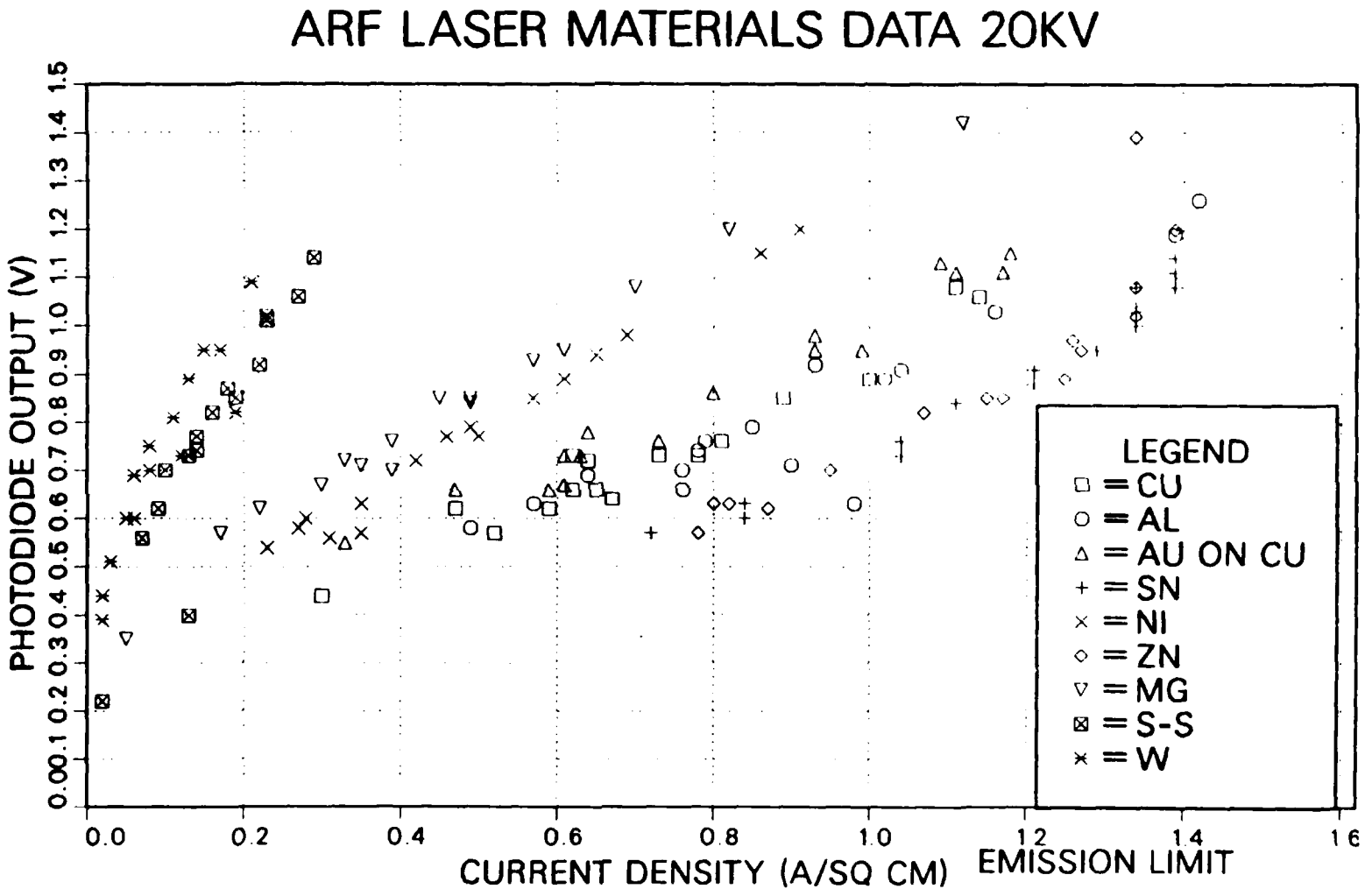

Figure 6. Nine Cathode Materials Plotted at 20KV, Showing Correlation of Photodiode Output to Computed Current Density Generated at the Collector.

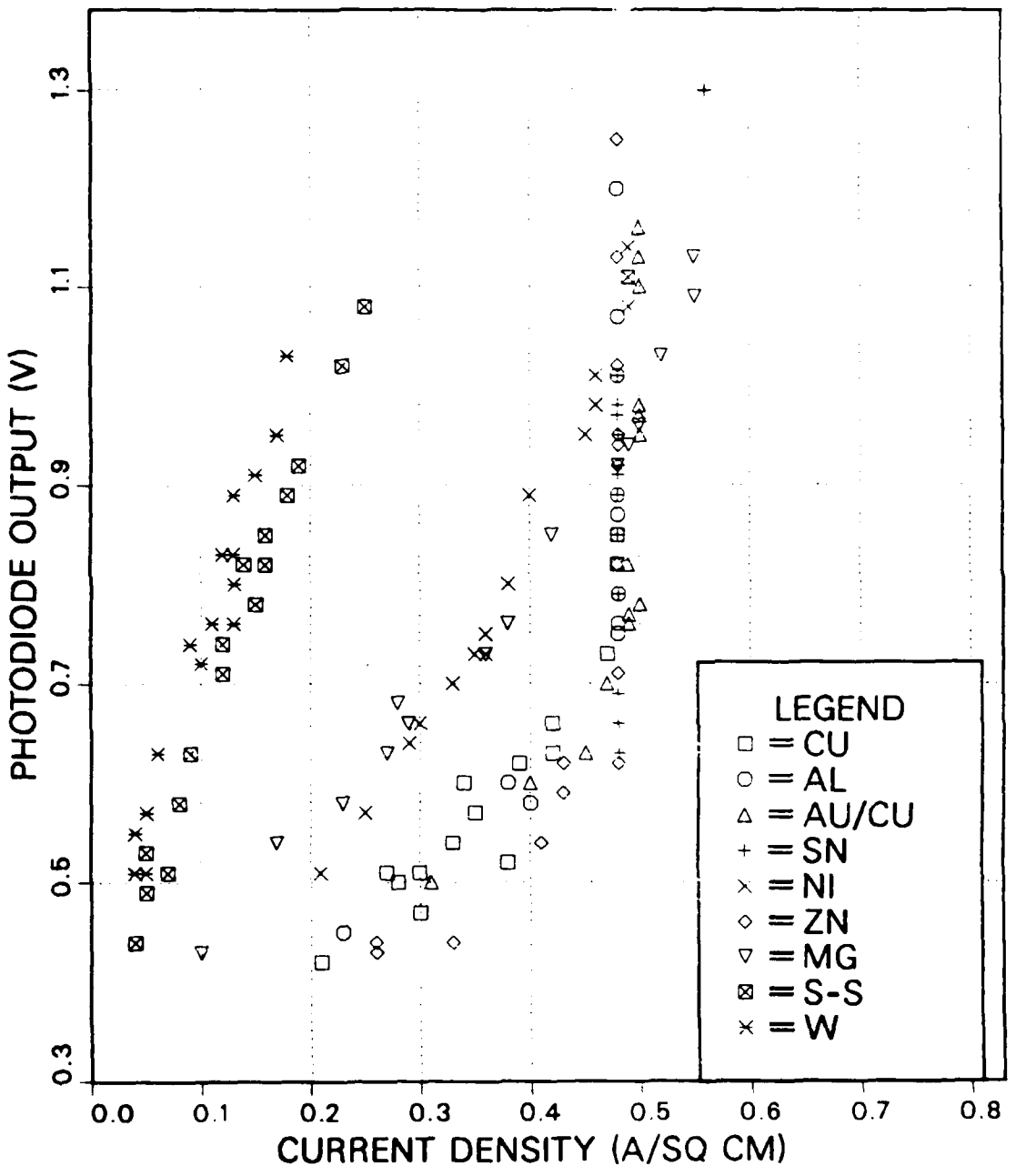

Figure 7. Nine Cathode Materials Plotted at 10KV, Showing a Linear Slope for Emission Limited Flow Changing to a Vertical Slope as Space Charge Limit is Reached.

reflectivity of the surface at the particular incident photon wavelength involved. An attempt was made to determine the absolute quantum efficiencies of the metal cathodes by using experimentally determined reflectivities. Cathode reflectivity was experimentally determined from the ratio of the measured incident energy normal to the cathode surface as compared to the measured energy reflected when the cathode was placed at 45 degrees to the incident path. This energy ratio was accomplished with a Gentec-200 calorimeter and had an accuracy of ±4%. The ArF laser was attenuated so that an average power of 100 KWatts/cm^2 was developed at the cathode surface when determining the reflectivity. The lower laser power was used to minimize pulse to pulse laser fluctuations inherent in this LAMBDA-PHYSIK laser at high power settings and also to reduce the possibility of plasma formation on the surface which could have affected the reflectivity calculations. Values for experimental reflectivity are listed in Table II.

As a quick comparison, theoretical values calculated using known reflectivity relationships and optical constants for the metals [Ref. 17] are also listed. These comparison values assumed a random polarization of the incident laser beam and a laser beam angle of incidence that was normal to the surface. Although this represents a 45 degree difference in incidence angle between the two values, the angular difference is deemed to have a small effect at this photon wavelength. Values not listed are due to lack of available optical parameters for calculations.

The experimental values for reflectivity show that in all but one case (aluminum) the reflectivities vary by just ±6% about an average

polarization and a 20% horizontal polarization. No attempt was made to fully polarize the laser beam horizontally, or vertically, to assess effects. It is probable that an increase in absolute quantum efficiency could be obtained with a laser beam that is totally horizontally polarized.

E. CHILD-LANGMUIR FLOW

It was observed that electron production as a function of accelerating potential applied to the anode-cathode geometry was consistent with the theoretical Child-Langmuir flow [Ref. 13] calculated for a planer diode arrangement. A predicted space charge limit on current density was calculated using the relationship:

$$J = K \frac{V^{1.5}}{d^2},$$

where J, K, V and d are the current in A/cm^2, perveance in $AV^{-1.5}$, accelerating potential in volts, and anode-cathode separation in centimeters. The assumed planer diode geometry uses a perveance (K) of 2.334×10^{-6} $AV^{-1.5}$ [Ref. 18]. Perveance is identified as a measure of the effectiveness in confining the space charge of the electron beam.

Experimental data for two copper cathode arrangements and the theoretical space charge limit are plotted in Fig. 9. It shows that the experimental output was slightly less in all cases over what is predicted from the space charge limit. This plot is based on the use of a copper cathode with the first experimental geometry but is representative of the response observed for each of the nine cathode metals used with the second geometry.

Additional factors considered that could have produced higher current densities in the experimental setup were ion production and secondary electron production due to electrons impacting the edge of the anode restrictive aperture. These contributions were not individually assessed in this experiment.

The fact that positive metal ions might be increasing current due to secondary electron generation after impact with the cathode surface was considered. However, the observed pulse shapes of the output current did not show any distortion nor any "tails" compared to the input laser pulse shape. The ions being heavier and slower would have added a delayed pulse shape distortion if present. None was observed.

In addition, secondary electrons generated from primary electron collision with the edges of the anode aperture would cause increased current with little alteration in output pulse shape and would have increased the observed difference in the experimental data and the theoretical space charge limit plotted in Fig. 9.

Excellent correlation between theoretical and experimental derived data plotted in Fig. 9, occurs when electron backscattering from photoelectrons impacting the collector surface is considered. The collector surface (center of the coax cable) was made of aluminum. From backscattering data run by a computer program [Ref. 19] at Los Alamos, we know that 20KV electrons impacting aluminum would produce about 15% backscatter. Lower energy, 10KV electrons would produce about 8% backscatter. These backscattered electrons are lost and do not contribute to the output voltage pulse, making the experimentally calculated photocurrent lower than its actual value. If just the

objective with the second geometry was to obtain a relative comparison of quantum efficiency for the metal cathodes and not to maximize current densities.

G. RELATIVE QUANTUM EFFICIENCY DETERMINATIONS

Relative quantum efficiencies are related to the experimental results only when emission limited data is considered. Relative quantum efficiencies experimentally determined at 20KV accelerating voltage are displayed in Fig. 10. Relative quantum efficiencies determined at 15KV accelerating voltage are shown in Fig. 11. These nine metals are further listed in Table I, in order of decreasing Q. E.. In general, the ordering was consistent between metal cathodes at the three accelerating voltages tested. Deviations were thought to be due to the pulse to pulse power changes in the laser which led to inaccurate power determinations. Quantum efficiencies (η) were calculated using the relationship:

$$\eta = 6.41 \frac{J}{P},$$

where J and P are the photoelectron current density in amps/cm^2 and power in Watts/cm^2 respectively. The constant 6.41 is the quantum energy (in electron volts) for a photon with a wavelength of 193.4 nm.

From Fig. 10, we note that the highest and lowest relative Q. E. are separated by about one order of magnitude between the nine cathode samples. The experimental accuracy in determining power allows at best a qualitative validity to these orderings. Comparisons between groups of metals as having a higher Q. E. can be recognized, but an absolute

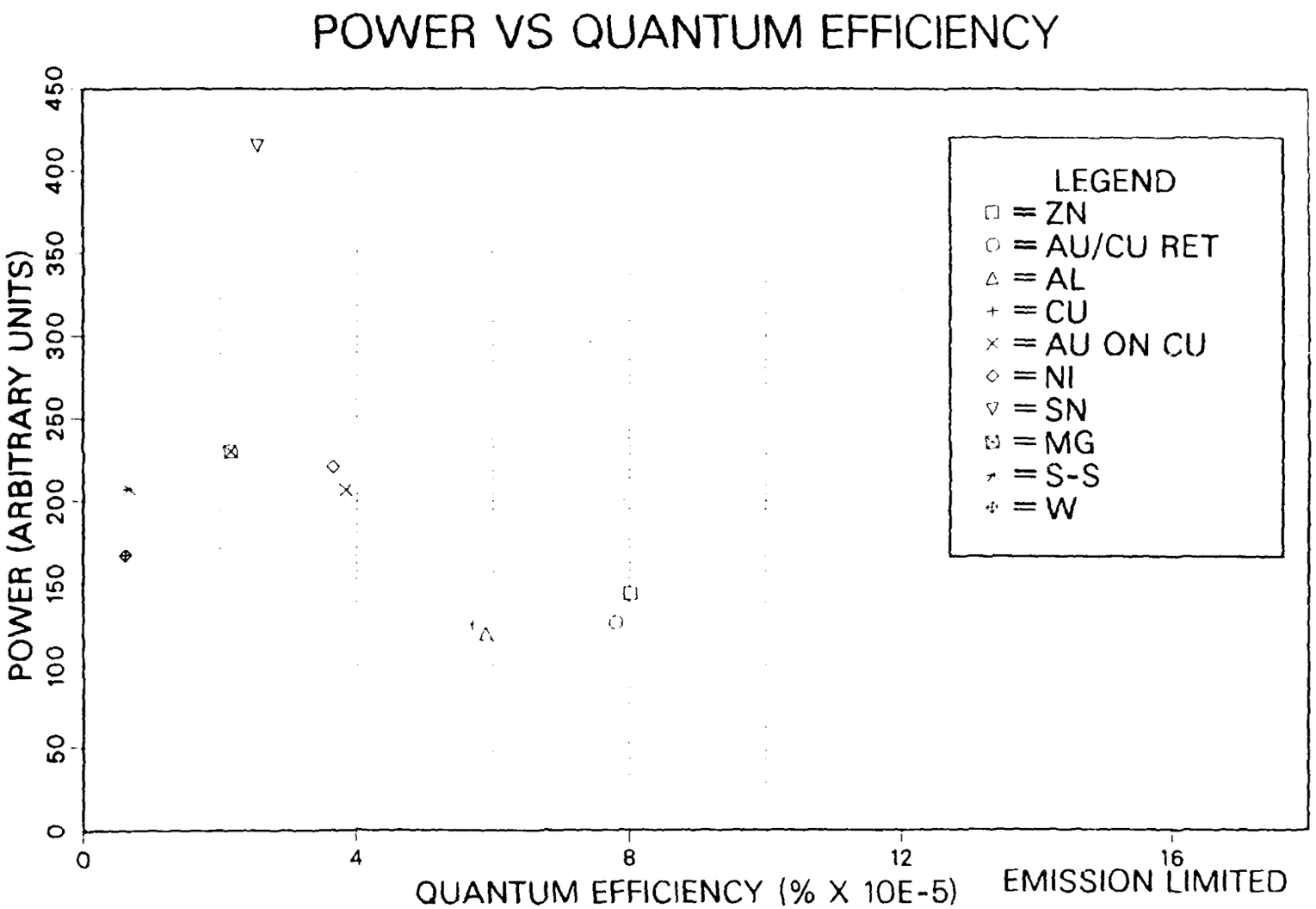

Figure 10. Relative Quantum Efficiency Comparison at 20KV Accelerating Voltage.

VI. CONCLUSIONS

Using an ArF excimer laser to generate "cold" photoelectrons, an experimental investigation was conducted on nine metal cathodes. The primary goal of the experiment was to perform a relative evaluation of the quantum efficiencies (Q.E.) for the metal cathode materials. Results showed, with an anode-cathode accelerating voltage of 20KV, that for the nine metals tested, zinc produced the highest quantum efficiency. Tin, aluminum, copper and gold followed as a group, and ranked higher as photoelectron emitters than nickel, magnesium, stainless steel and tungsten as a group. It must be remembered that these are relative rankings and that the actual quantum efficiencies of metals are generally poor. Attempts to calculate relative quantum efficiencies produced values for the nine metals that range from 2×10^{-4} to 1×10^{-5}. These values are lower than the generally agreed maximum value of 10^{-2} obtainable with 10 e.v. photons and pure metals but do closely approach the general Q.E. value of 10^{-4} for metals. As calibration of the laser pulse power was not very reliable, experimental calculation inaccuracies could account for the apparent disparity in these efficiencies. Furthermore, if reflectivities are taken into account, then Q.E. may be compared favorably to accepted values in the 10^{-2} to 10^{-4} region for metals.

Additional results demonstrated a current density of 91 A/cm^2 could be achieved with a copper cathode at 29KV accelerating potential. Reflectivity determinations indicated that only aluminum had a

VII. SUGGESTED FOLLOW UP EXPERIMENTATION

Investigations into the more efficient utilization of the laser pulse could be made. Determining the minimum power requirements for electron production would also be valuable information. This would entail an experimental setup to determine the laser pulse power on an absolute scale.

The two photon excitation concept may be a method to improve the coupling of photon energy delivered to the cathode. Using attenuated total reflection (ATR) [Ref. 21], which uses two cathode plates placed at 90 degrees to each other, an increase in photoelectron quantum efficiency may be possible. However, because this would involve a change in the planer geometry arrangment, it may detrimentally alter the electric fields between anode and cathode and adversely affect the electron beam quality.

Since photoemission depends on the photon energy, $\hbar\omega$, and the electronic structure of the cathode material, an investigation to locate a resonance in one of the more efficient metal cathodes might be made to increase the quantum efficiency. Resonances are associated with the electronic shell structure of the cathode material. A resonant frequency for the incident photon energy could be found by varying the incident photon frequency with a tuned dye laser.

APPENDIX B

LIST OF EQUIPMENT

Osciloscopes: Techtronics R-7103, 1GHZ
Vertical Base 7A29
Horizontal Time Base 7B15

DC Power Supply: Hipotronics Power

Laser: LAMBDA PHYSIK EMG 150T

Laser Variable Attenuator: NRC Model 935-10

High Vacuum Pump: CTI Cryogenics, Cryo-Torr-8

Photodiode: Hamamatsutu R1193U-04

Calorimeter: Gentec-200

Photodiode: EG and G Electronics FND-100Q

Photodiode Power Supply: BNC Portanim Model AP-3

Boxcar Averager: EG and G Princeton Applied Electronics Model 162

LIST OF REFERENCES

1. Lee, M. and Reifenberger, J. C., "Periodic Field Dependent Photocurrent from a Tungsten Field Emitter", Surface Science, v. 70, pp. 114-130, 25 April 1977.

2. Sommer, A. H., Photoemissive Materials, pp. 15, 19, 21-26, 33, 57-174, Robert E. Krieger Publishing Co., 1980.

3. Burroughs, E. G., "External Field Enhanced Photoemission in Silver-Cesium Oxygen Photocathodes", Applied Optics, v. 8, no. 2, pp. 261-265, February 1969.

4. Lee, C. H., Oettinger, P. E., Pugh, E. R., Klinkowsstein, R., Jacob, J. H., Fraser, J. S., and Sheffield, R. L., "Electron Emission of over 200 A/cm^2 from a Pulsed-Laser Irradiated Photocathode", IEEE Transcripts on Nuclear Science, v. 32, pp. 3045-3047, October 1985.

5. Walldeim, L., "Surface Photoelectric Effect for Thin Metal Overlays", Physics Letters, v. 54, pp. 943-946, 4 March 1985.

6. Bergland, C. N. and Spicer, W. E., "Photoemission Studies of Copper and Silver: Theory", Physics Review, v. 136, pp. 1030-1044, 16 November 1964.

7. Bergland, C. N. and Spicer, W. E., "Photoemission Studies of Copper and Silver: Experiment", Physics Review, v. 136, pp. 1044-1064, 16 November 1964.

8. Seitz, F., The Modern Theory of Solids, p. 139, McGraw Hill Book Co., 1940.

9. Feuerbacher, B., Fitton, B., and Willis, R. F., Photoemission and the Electronic Properties of Surfaces, pp. 3, 12, John Wiley and Sons, Inc., 1978.

10. Cardona, M. and Ley, L., Topics in Applied Physics: Photoemission in Solids I, v. 26, pp. 2, 21, 57, Springer-Verlag Co., 1978.

11. Gudat, W. and Kunz, C., "Close Similarity between Photoelectric Yield and Photoabsorption Spectra in the Soft-X-Ray Range", Physical Review Letters, v. 29, p. 170, 17 July 1972.

12. Barton, J. J., "Direct Surface Structure Determination with Photoelectric Diffraction", Physics Letters, v. 51, pp. 272-275, 25 July 1983.

BIBLIOGRAPHY

Kittel, C., Introduction to Solid State Physics, 2nd ed., John Wiley and Sons, 1956.

Koller, L. R., The Physics of Electron Tubes, 2nd ed., McGraw-Hill Book Co., 1937.

Miller, R. B., An Introduction to the Physics of Intense Charged Particle Beams, Plenum Press, 1982.

Nagy, G. A. and Szilagyi, M., Introduction to the Theory of Space Charge Optics, Wiley Publishing, 1974.

Pierce, J. R., Theory and Design of Electron Beams, 2nd ed., D. Van Nostrand Co., 1954.

Zaidel, A. N. and Shreider, E. Y., Vacuum Ultraviolet Spectroscopy, Humphrey Science Publishers, 1970.

END

11-87

DTIC